

FINITE ELEMENT MODELING OF ADJACENT PRESTRESSED CONCRETE BOX BEAMS

Eric Steinberg, PhD, PE, Professor, Civil Engineering, Ohio University, Athens, OH

Jonathan Huffman, Bridge Engineer, GPD Group, Columbus, OH

John Ubbing, Grad. Research Asst., Civil Engineering, Ohio University

Oliver Giraldo-Londoño, Grad. Research Asst., Civil Engineering, Ohio University

ABSTRACT:

Several finite element models were constructed to study aspects that influence the interaction between adjacent beams. Shear key size, shape, material, bond characteristics, transverse ties, dowel bar effects, thermal gradient effects, and beam alignment were analyzed parametrically to determine how each mechanism effects load transfer between adjacent beams.

Three finite element models were created for this study. The first model consisted of two beams joined with dowel bars and partial depth shear keys with conventional grout. This model was used to study transverse ties and thermal effects. The second model considered two shear key shapes with two different grout materials. This model utilized partial and full depth shear keys with both conventional grout and UHPC. In the model, dowel bars were placed in the shear key. The third model was a full-scale bridge with the beams positioned to align with the crown of the road way.

From the modeling, it was determined which practices and/or combinations of the shear key size, shape, material, dowel bars, and beam orientation will yield the most sufficient load transfer mechanism. The modeling also investigated the effect of temperature gradient within the box beams on shear key performance.

Keywords: Bridge Modeling, Finite Element Modeling, UHPC

INTRODUCTION:

Adjacent box beam bridges have been commonly deployed around the US as an economical structure type for short to medium spans, but have been shown to be susceptible to degradation as a result of poor longitudinal connection performance. Longitudinal Ultra High Performance Concrete (UHPC) shear keys have been implemented recently in bridges in Ontario, Canada. However, little to no data on the actual performance of these connections as well as their design has been collected. Several finite element models of different adjacent box beam systems were constructed to study various aspects of the transverse load transfer mechanisms. The design features studied in this modeling included full and half depth shear keys, transverse ties, conventional grout with post-tensioning, UHPC grout, staggered dowel bars, thermal gradient effects, and a full scale bridge.

UHPC is becoming an option for use as an improved construction material and has garnered interest around the US, but is still in its infancy in terms of deployment in bridge design. Developed in France in the 1990's, this material retains superior mechanical and durability properties. UHPC has been found to have a compressive strength greater than 21.7 ksi and a modulus of elasticity greater than 7,600 ksi^[1]. In the United States, UHPC has been utilized in Iowa, New York, and Virginia for multiple bridge components such as waffle slabs, pi-shaped girders, and field-cast connections^{[2][3][4]}.

A first model was created to study the load transfer mechanism between adjacent box beams using the typical longitudinal shear key. This is critical for evaluating and load rating these bridges and to have a better understanding of existing designs. The model consisted of two adjacent box beams connected by a shear key and transverse ties located at third points along the bridge span. The beams studied were taken from a previously modeled adjacent box beam bridge^[5]. In this model the effect of the temperature gradient of the beams on load transfer was examined. Also, the effect the magnitude of post-tensioning has on transverse load transfer was investigated. The effects of positive and negative temperature gradient included in this model were according to AASHTO LRFD^[6].

The second FE model was created to compare results with full scale tests being conducted at the Federal Highway Administration's (FHWA) Turner Fairbank Highway Research Center (TFHRC) and to analyze changes in parameters. When analyzing results, a majority of the technical focus will be placed on the performance of the full and half depth UHPC shear keys as well as the shear resisting dowel bars in each keyway. Results will be used to aid in the design of an adjacent prestressed concrete box beams bridge in Fayette County, Ohio that will utilize UHPC in the longitudinal connections.

A full bridge model was also completed for the future Sollars Road Bridge in Fayette County, Ohio. The existing Sollars Road Bridge is due to undergo a full substructure and super structure replacement in the summer of 2014. The new bridge will be a 61' long single span box beam bridge. In an attempt to enhance the effectiveness and design life of the shear key, the conventional grout of the shear keys will be replaced with UHPC. Dowel bars will

also be placed within the precast beams and will protrude into the shear key. Once the box beams are fit up and the UHPC shear keys have been poured, the dowel bars will assist in the load transfer between beams.

The Sollars Road Bridge model utilized seven of Ohio's conventional B21-48 box beam with modifications to the shear key detail to incorporate the shear key shape being tested by FHWA. The shear key material used for this model was UHPC and dowel bars were placed within the shear keys and beams. Each beam possessed 24 - ½" diameter 270 grade, low relaxation, prestressing strands, and 6 – Grade 60 #5 bars. The modeled bridge was loaded to simulate four tandem axle dump trucks. The effects of the prestressing and self-weight on the beams were also incorporated into the loading of the bridge.

MODEL CONSTRUCTION:

All of the finite element models were created with Abaqus/CAE and were analyzed as either linear or non-linear three-dimensional models. The first model was constructed to perform a study involving the effects transverse tie post tensioning and the temperature on the load transfer behavior between typical adjacent box beams. The second model was created to simulate experiments being conducted by FHWA, where the shape and material of the shear key are being investigated. The third finite element model, generated to represent the future Sollars Road Bridge, takes into account the non-linear material properties of the concrete superstructure and the transverse load transfer mechanisms to capture the global behavior of the bridge under various truck loadings.

TEMPERATURE MODEL

The model consisted of two adjacent box beams connected through a shear key, and transverse ties located at third points along the bridge span. The beam shapes were modeled similar to beams previously model for bridge FAY 35-17-6.80 in Fayette County, Ohio ^[5].

The model was assembled using five different parts: box-beams, shear key, longitudinal reinforcement (prestressed and conventional), diaphragms, and transverse tie rods. The beam sections as well as the shear key and longitudinal reinforcement were extruded 47'10" to model the bridge's span ^[5].

Materials

All parts were modeled as non-linear elastic. The Young's modulus and Poisson's ratio were used to define the linear properties for all materials. A summary for the linear elastic material properties for all parts used in the model is shown in Table 1.

Table 1 - FEM Material Properties

Part	Young's modulus (ksi)	Poisson's ratio
Beams	5000	0.2
Shear key	5000	0.2
Prestressing strands	28500	0.3
Transverse ties	28500	0.3

Mild steel	29000	0.3
------------	-------	-----

To define the plastic behavior of the materials, a set of values containing the true plastic stress and the true plastic strain was input. Stress-strain relationships for both concrete and steel are shown in Figures 1 and 2, respectively. It is important to note that tensile and compressive behavior for all materials was assumed to be the same.

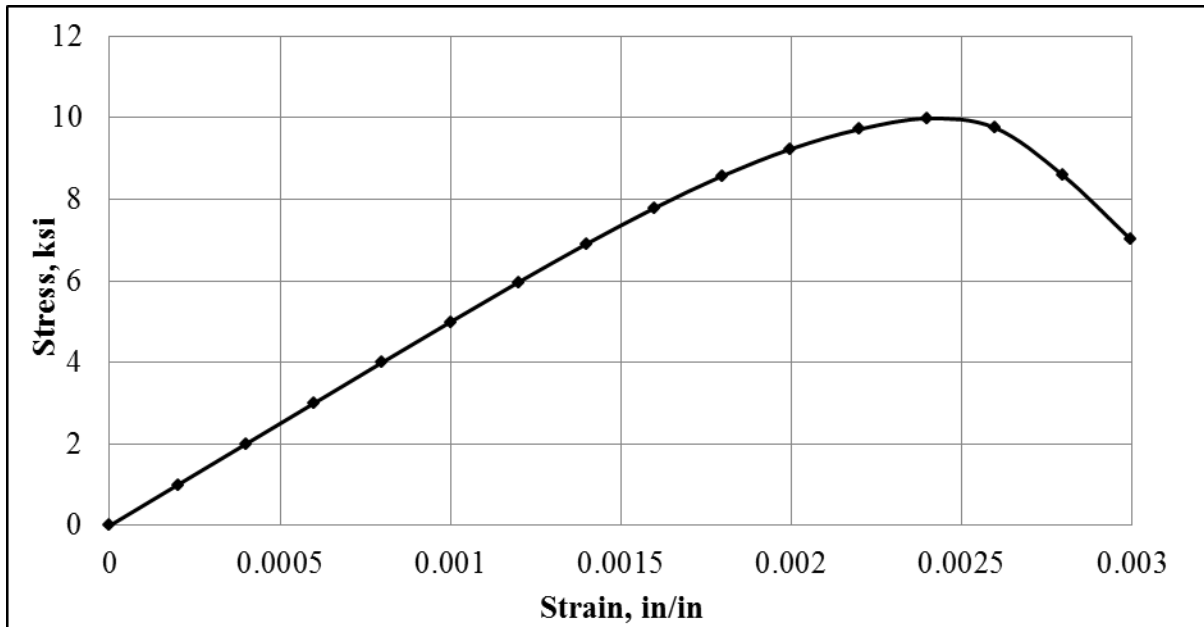


Figure 1 - Stress-strain relationship for concrete

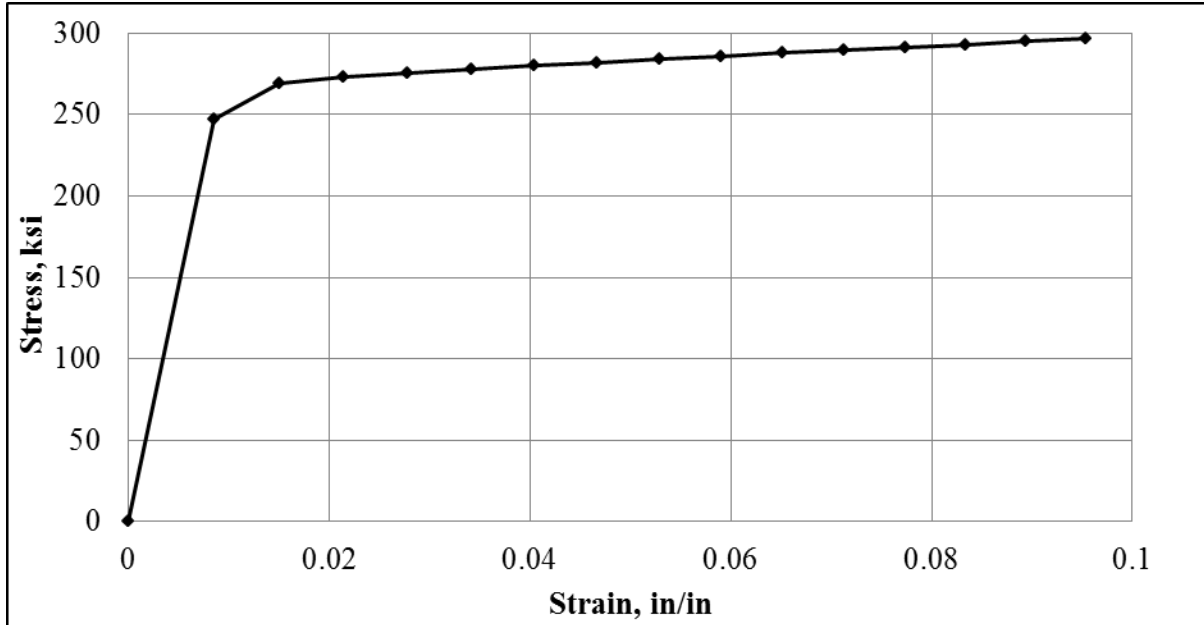


Figure 2 - Stress-strain relationship for prestressing steel

Boundary Conditions & Interactions

The bridge was modeled as simply supported. One of the ends was fixed against translation in all directions. The other end was fixed against vertical and transverse translation, but was free to move longitudinally. No rotational restraints were imposed. These restraints were imposed on the bottom edge at the ends of the beams.

The interaction between the longitudinal reinforcement and the box-beams was modeled as an embedment constraint. The interaction between the beams and the diaphragms was modeled as a tie constraint. This prevents any movement between the diaphragms and the beams^[5]. When defining the interaction between the beams and the shear key, a surface-to-surface contact behavior was used. This behavior was divided into normal and tangential behaviors. The normal behavior was modeled with a linear pressure-overclosure relationship between the two surfaces in contact. The selected contact stiffness for the normal behavior was appropriately selected in order to minimize the penetration between two surfaces in contact. The contact stiffness used in the models was 10 ksi/in. The tangential behavior was defined using the Coulomb friction model with a limit on the critical shear stress. The magnitude for the critical shear was chosen as 0.8 ksi according to results of numerous slant shear tests^[7]. The friction coefficient used in the model was $\mu = 0.8$ according to typical values of concrete-to-concrete friction coefficients.

Loading

To analyze the load transfer mechanism between the two beams, one of the beams was loaded with the AASHTO LRFD design lane load plus the HL-93 wheel loads, as shown in Figure 3. For this model, a transverse post-tensioning (TPT) force was applied only at third points along the bridge span. The TPT force was varied from 0 kips to 80 kips in order

to analyze contribution of the TPT in the performance of the load transfer mechanism. To model the transverse post-tensioning force, a negative temperature was applied to the tie rod using a predefined field. The temperature required to reach the TPT was obtained by evaluating the thermal stress assuming the transverse ties to be fixed at the ends. That is

$$\Delta T = -\frac{TPT}{\alpha EA_t}$$

where: α = Thermal expansion coefficient for steel = $5 \times 10^{-6}/^{\circ}\text{F}$;

E = Young's Modulus for steel = 28500 ksi ; and

A_t = Area of transverse tie rod = 0.785 in^2

To prevent issues of straining perpendicular to the transverse tie due to the applied temperature, orthotropic thermal properties were assigned to the steel used for the transverse ties. The thermal expansion coefficient was set to zero in the directions perpendicular to the transverse tie, and set to $5 \times 10^{-6}/^{\circ}\text{F}$ in the longitudinal direction of the bar. In addition, a temperature gradient as suggested by AASHTO LRFD was applied to the models. Figure 3 shows the positive temperature gradient. The negative temperature gradient is -0.3 times the positive gradient.

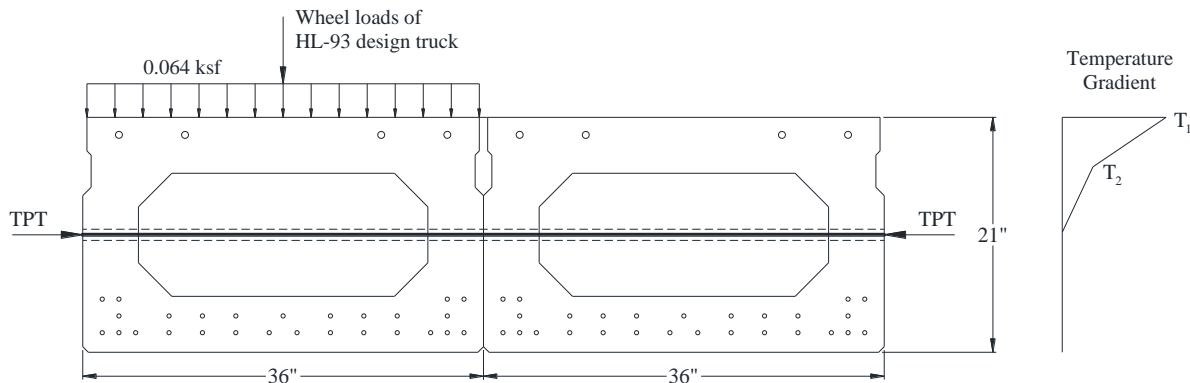


Figure 3 - Loading procedure for the Temperature Model

UHPC MODEL

Models were constructed for each type of shear key using Abaqus/CAE based on drawings provided by TFHRC. Each beam was composed of solid, deformable, three dimensional parts that were assigned elastic properties that reflect typical steel and elastic concrete behavior and previous testing done on UHPC. Two beams were modeled instead of a full bridge width in order to directly model the FHWA testing.

Both box beams utilized either a partial or full depth shear key filled with conventional grout (Figure 4), included a 50ft span complete with four diaphragms, the longitudinal reinforcement, and eight post tensioning points. In the finite element model (FEM), steel elements were embedded into each concrete beam and effects of debonded

strands were included for eight of the upper tensile reinforcement strands by simply shortening each strand by the specified debonded length (either six or ten feet).

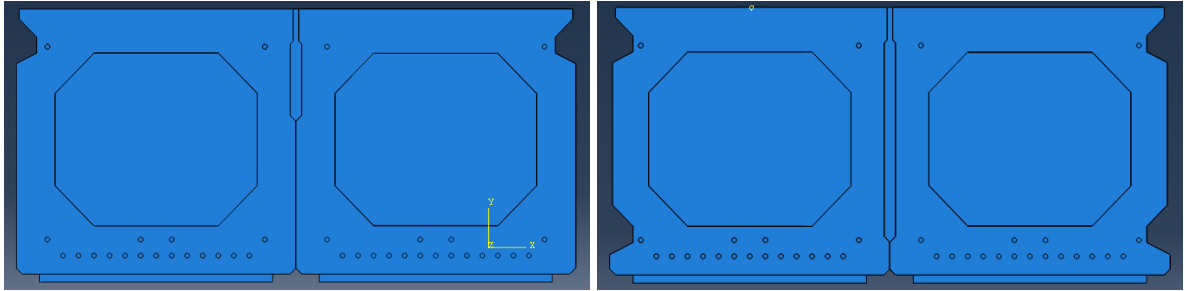


Figure 4: Partial & Full Depth composite box beam with conventional grout

Unlike the temperature model, transverse post tensioning was applied at both ends of the pair of beams as well as the third points. To model the force of post-tensioning along both beams, four pairs of concentrated forces were applied on the exterior of each beam near the middle of each diaphragm (Figure 5). Four sets of springs in the same location along the length of the beam were used to model the post-tensioning tendons through the shear key.

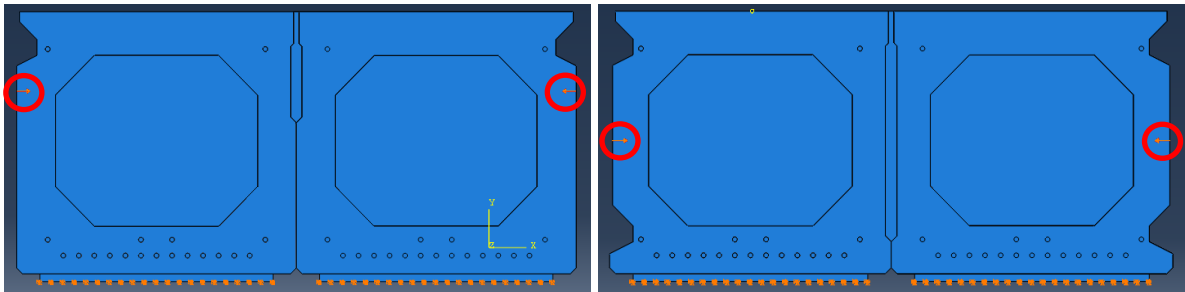


Figure 5: Post-tensioning locations in partial and full depth conventional grout beams

The two models utilizing UHPC did not include post tensioning due to staggered dowel bars located in the widest opening of each shear key (Figure 6). These #4 bars were embedded 18" into each beam and protrude 5.5" into the shear key serve as shear-resisting components. Other than dowel bars, a modified shear key shape, and no transverse post-tensioning, the models with UHPC were the same as the grouted beams.

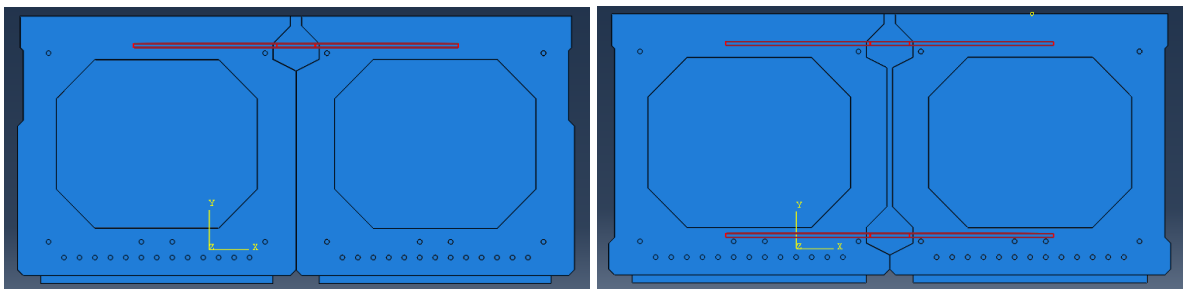


Figure 6: Partial and full depth composite box beam with UHPC grout

Materials

Each composite box beam was composed of concrete with an average compressive strength of 9830 psi (provided by TFHRC), which according a reinforced concrete design source, would result in a modulus of elasticity of 4,966 ksi^[8]. This value was assigned to each normal weight concrete component along with a Poisson's ratio of 0.2. The conventional grout material was also assigned a modulus of elasticity of 4,420 ksi and a Poisson's ratio of 0.2. The two models incorporating UHPC shear keys had an elastic modulus of 7,600 ksi and a Poisson's ratio of 0.18^[11].

Boundary Conditions & Interactions

In order to restrain the beams in a manner similar to the FHWA testing, neoprene pad parts were created and tied to each end of each beam. Each pad was 1" x 12" x 36" and had a modulus of elasticity of 30 ksi along with a Poisson's ratio of .499^{[6][9]}.

The bottom of the pads at one end of the beams were then assigned boundary conditions that restrained translations in the transverse and vertical directions, while the other pair of pads on the opposite end restrained translations in all directions.

Loading

Once the models were constructed, a loading procedure was created for each model to replicate the TFHRC's loading. This involved specifying four load distribution areas (two/beam) approximately 12"x12." As seen in Figure 7, the loading was positioned near the edge of each beam and approximately at midspan.

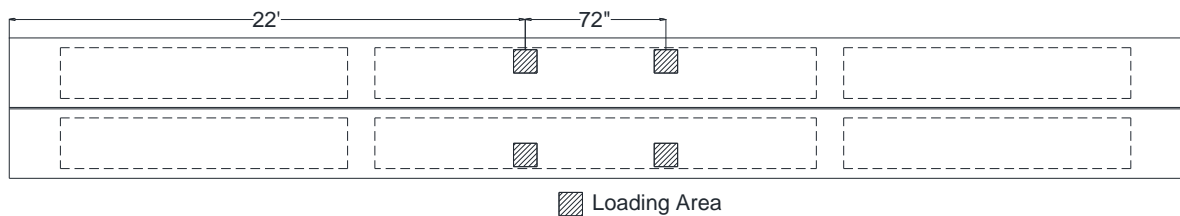


Figure 7: Loading locations along composite beams

The actual loading procedure followed an opposing cyclic pattern on each beam. For example, when the one beam was loaded at the smallest magnitude, the other beam would be loaded the largest magnitude. Figure 8 shows the opposing cyclic loading on each beam. This loading procedure was devised to test the shear key strength and durability.

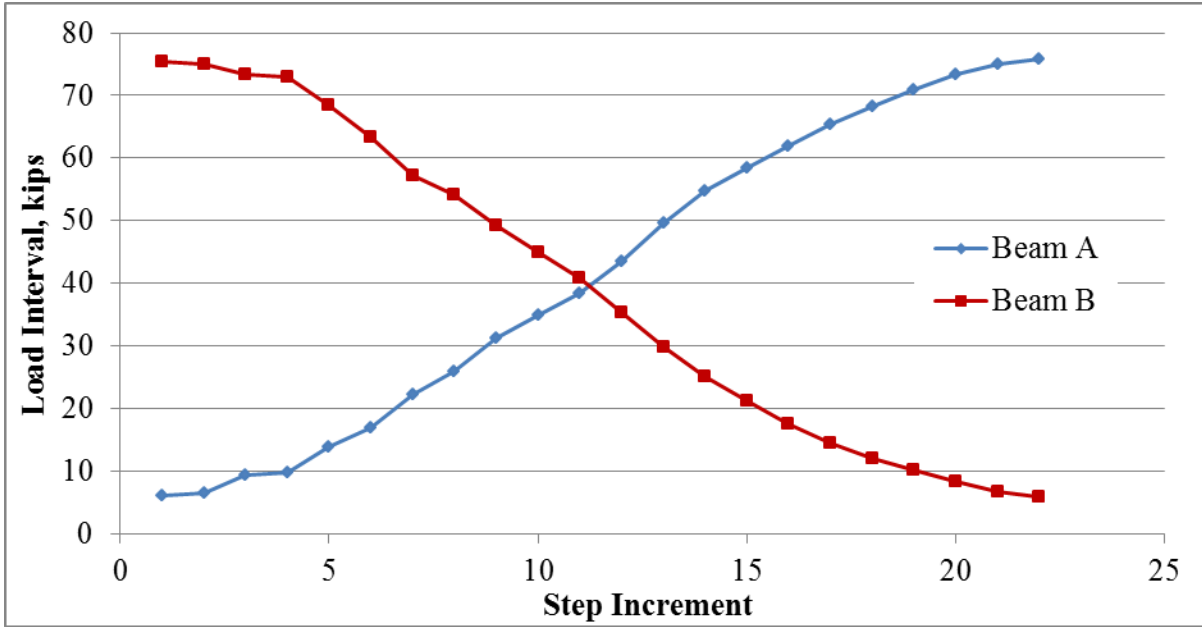


Figure 8: Cyclic loading procedure followed in finite element modeling

SOLLARS ROAD BRIDGE MODEL

The Sollars Road Bridge model consisted of seven, 61’ long, precast prestressed adjacent box beams with prestressed and conventional longitudinal reinforcement. The cross-sections of the box beams were drawn according to ODOT specifications for the B21-48. However, the shape of the shear key was modified to the shear key used in the FHWA testing. The box beams were aligned to match the slope of the asphalt overlay at 0.208%. This detail and the modeled strand pattern were specified in the preliminary bridge design specifications. Figure 9 shows the cross-sectional dimensions of the box beams with the reinforcement pattern and the shear key dimensions.

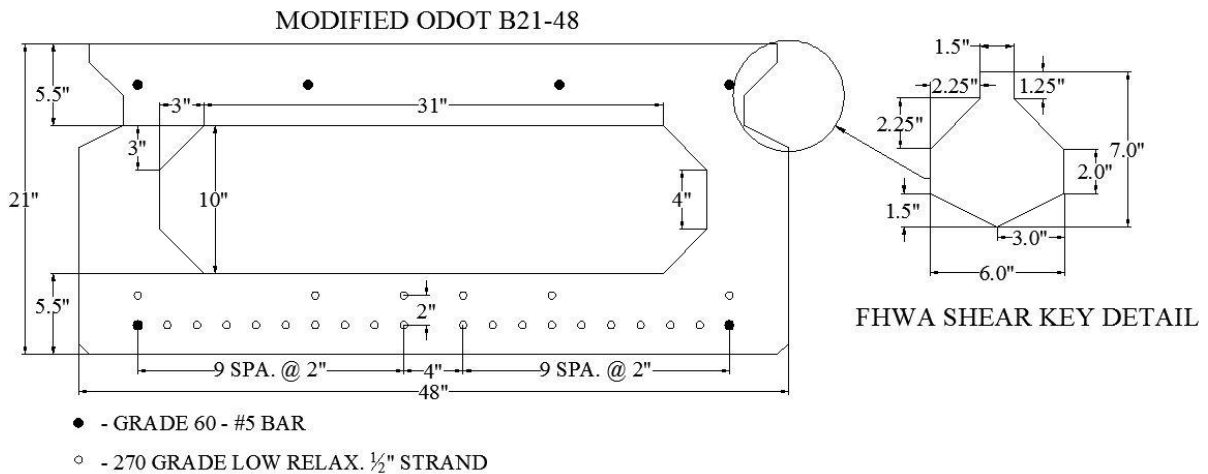


Figure 9 - Modified ODOT B21-48 with FHWA Shear Key Detail

The FHWA shear key detail shown in Figure 9 is considerably wider than the traditional shear keys. This was to allow adequate development of the transverse dowel bars that were embedded into the box beams. The dowel bars explained for the UHPC Model were also used in this model. However, the bars were staggered between adjacent beams resulting in a 6" c/c spacing between bars. The transverse dowel bars were used to replace the traditional transverse bars that run through the box beams.

Materials

The prestressed precast adjacent box beams were modeled with a concrete material that acts perfectly plastic after yielding. This concept is commonly used when modeling the post yield behavior of ductile metals, such as steel. However to allow for quicker convergence, the concrete adjacent box beams and UHPC shear keys were also modeled in this manner. It was not expected that this modeling technique would have a significant effect on the global behavior reflected in the model. This assumption was confirmed once the analysis was finalized. Also, the concrete and UHPC material properties were defined to act perfectly plastic for the tensile and compressive yield criteria. The materials were to continue to act perfectly plastic until a strain ten times the yield strain was reached, in which case the material failed. In this case, the concrete of the superstructure had a specified compressive design strength of 4.5 ksi. From relationships previously derived ^[5], the modulus of elasticity and tensile capacity of the concrete were determined from the compressive strength. From testing conducted by FHWA on the strength of the UHPC, the compressive strength was taken as 24 ksi, the tensile strength was 1.2 ksi, the modulus of elasticity was 7,600 ksi, and Poisson's ratio was 0.18 ^[1]. Similar to the concrete, the UHPC was defined as perfectly plastic until a strain ten times the yield strain was achieved. The stress-strain diagram for the concrete and UHPC are shown in Figure 10.

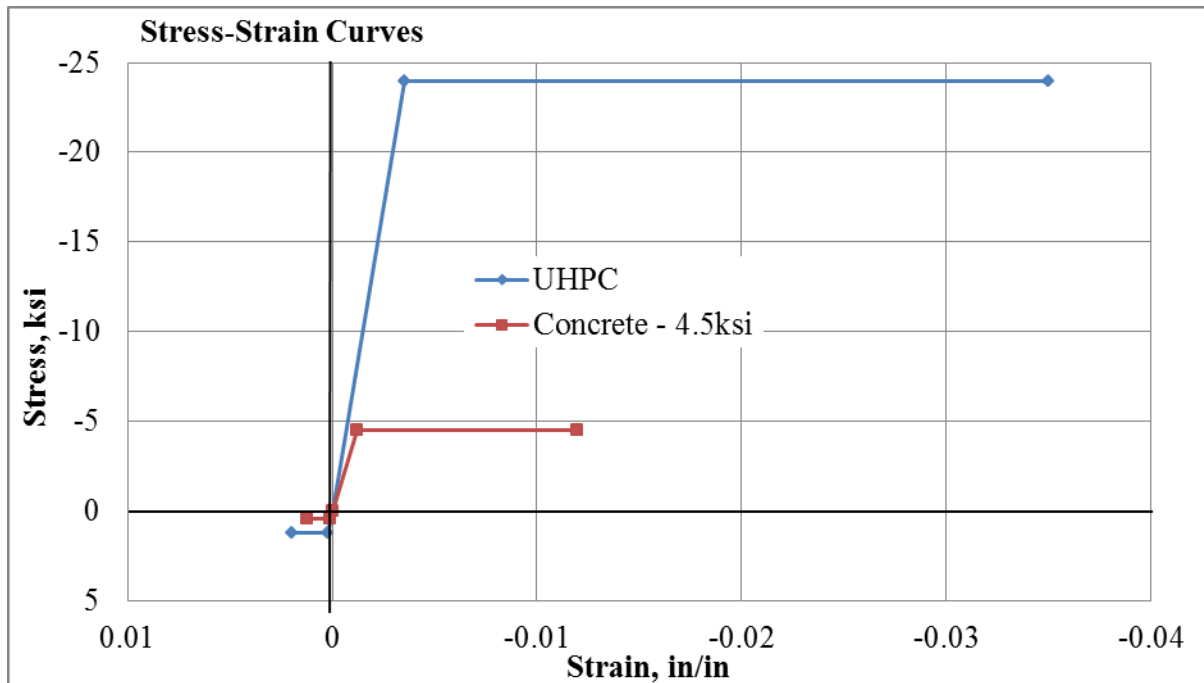


Figure 10 - Stress-Strain Diagram for the Concrete and UHPC

The steel components were modeled using traditional steel material properties. The prestressing strands were assigned a yield strength of 270 ksi, a modulus of elasticity of 28,500 ksi and a Poisson's ratio of 0.3. The conventional steel reinforcement and transverse dowel bars were assigned a yield strength of 60 ksi, a modulus of elasticity of 29,000 ksi and a Poisson's ratio of 0.3. These materials were defined to act as perfectly plastic once the yield conditions were reached.

Boundary Conditions & Interactions

To achieve a representative model, the bearing pads between the abutments and box beams were also included in the model. The bearing pads were assigned the same materials as the bearing pads described for the UHPC Model. In the model, the bearing pads represent a combination of a rotational spring and a translational spring at the ends of the beams. This allows the beams to rotate as they would in the field. It was assumed that the abutment will act as a stiff, rigid member and therefore the bottom sides of the bearing pads were fixed.

The steel reinforcement was modeled using the embedment constraint ^[10]. This assumes there was no slip between the steel and the concrete. The prestressing in the stands was also included in the model. This was achieved in the same manner as described previously with the Temperature Model.

The interaction between the concrete beams and the UHPC shear keys was modeled using a surface to surface contact. The tangential and normal behaviors of the contact were defined by defining the coefficient of friction (μ) and contact stiffness (k) between the two materials. The normal behavior controls the transfer of stresses between the two surfaces and also restrains the nodes of the two contacting surfaces from penetration into one another. For this model the coefficient of friction was chosen to be 0.8 and the contact stiffness was assigned as 50 ksi/in. When testing is conducted on the actual bridge these values will be changed to more accurately represent the load transfer behavior of the adjacent box beams.

Loading

There were two separate loadings modeled on the bridge. The dimensions and tire loads were approximated from previous testing that has been conducted in Fayette County, Ohio ^[11]. It was projected that the trucks used in the testing of the future Sollars Road Bridge will be similar to the trucks previously used. For the two loading conditions, the same truck dimensions and tire loads were used for all four trucks. Each front axle tire load was 7.25 kips and each rear axle tire load was 10 kips. The first loading simulated four tandem axle dump trucks parked back to back positioned around the center of the bridge (Figure 11). The second loading was similar to the first, however in this loading case the trucks were shifted to one side of the bridge (Figure 12).

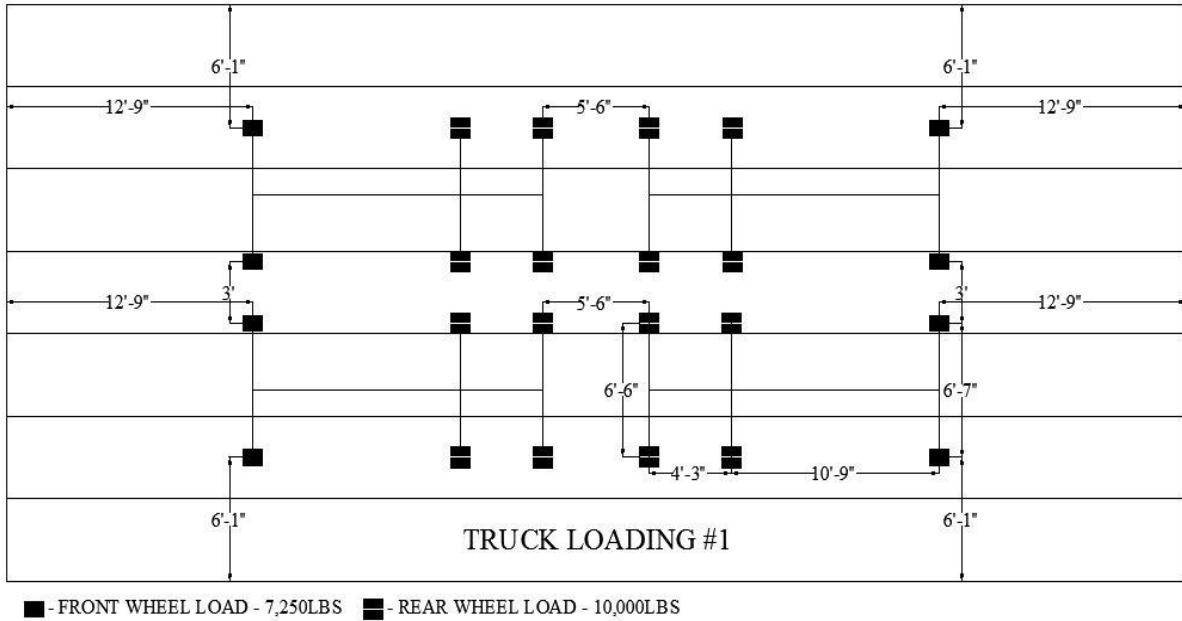


Figure 11: Truck Loading #1

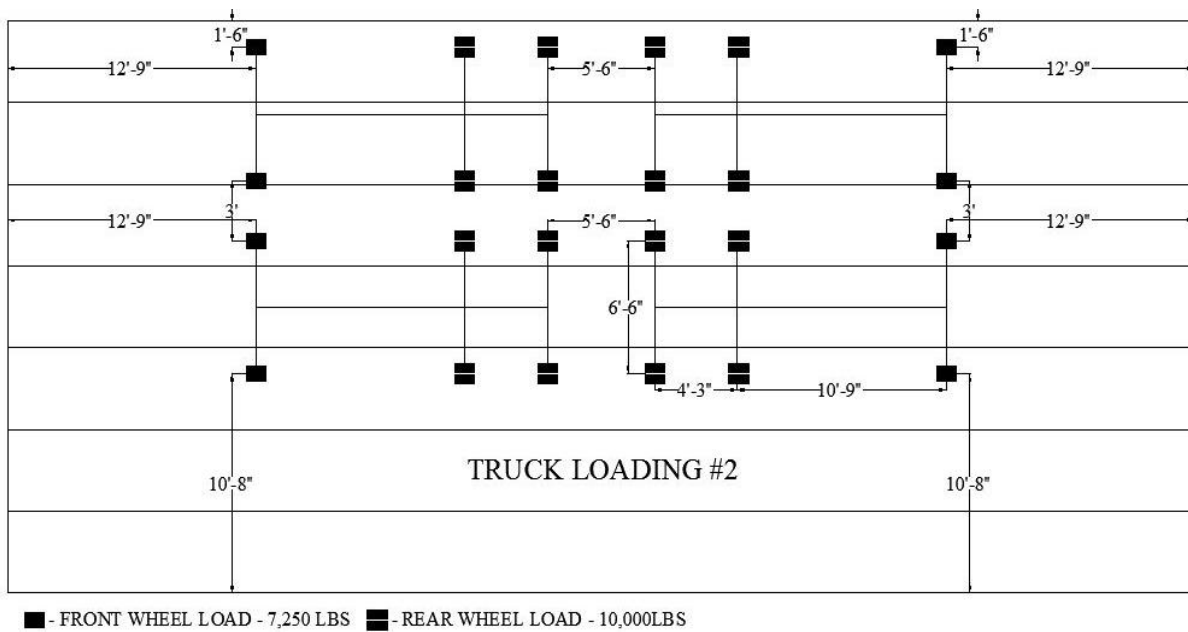


Figure 12: Truck Loading #2

To achieve a comprehensive model of the Sollars Road Bridge the prestressing forces in the strands and self-weight of the superstructure were also included in the finite element analysis. The prestressing was accounted for in the same manner as discussed previously for the temperature model. The stress in the strands after losses was anticipated to be 175 ksi. The effect of the self-weight was modeled by applying a volumetric body force on each concrete and steel part. The unit weight was assumed to be 145 lbs/ft³ for the concrete

components and the 490 lbs/ft³ for the steel components. Also, the unit weight of the UHPC was assumed to be the same of the normal weight concrete.

RESULTS:

TEMPERATURE MODEL

Once the model was loaded with the live loads, several analyses were performed with different amounts of transverse post-tensioning force. For each model, the differential deflection between the two beams was obtained at several locations along the bridge span. Figure 13 shows the differential deflections obtained at $L/6$, $L/3$, and $L/2$ along the bridge span. The results indicated that the differential deflections became smaller as the transverse post-tensioning force was increased. It was noticed that for TPT larger than 20 kips per diaphragm, there was no significant changes in the differential deflection. When friction between the two beams below the shear key was considered, a TPT force of 10 kips was sufficient to decrease the differential deflection to 0.02 in. This means that the differential deflection was reduced to 20% to 35% of the value obtained for zero TPT. Effects of temperature gradients were not shown in Figure 15, because they have a negligible effect in differential deflections.

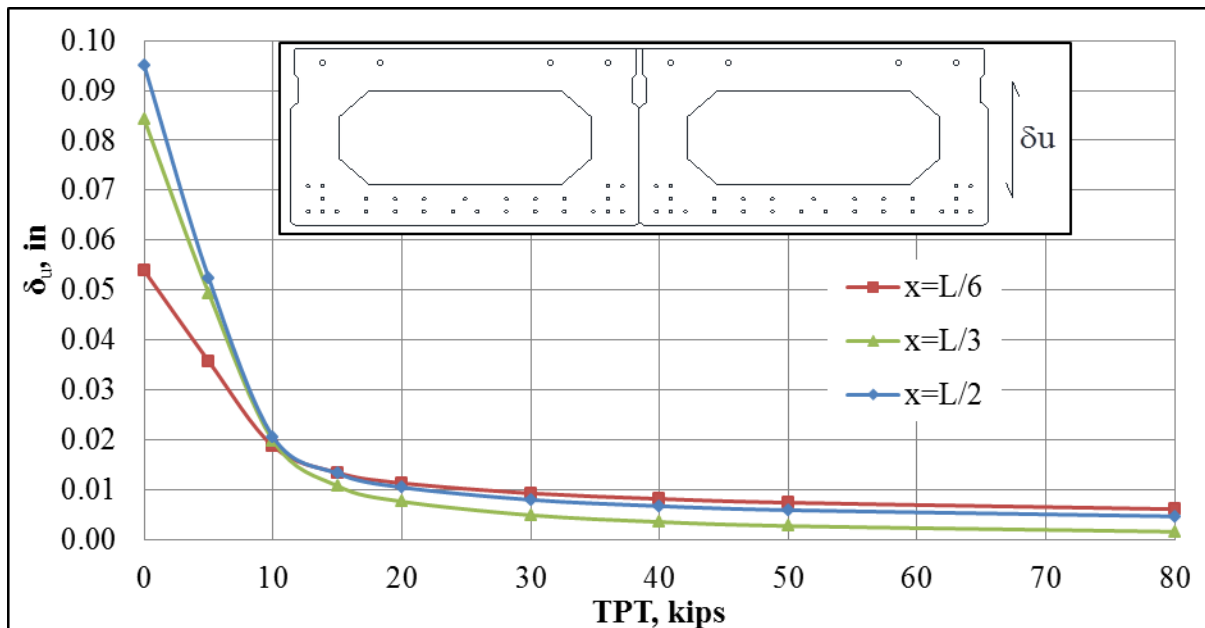


Figure 13 - Differential deflections between the beams verse TPT

The maximum tensile and maximum compressive stresses in the shear key were also recorded as the transverse post-tensioning force was varied. Figure 14 shows the maximum tensile stresses in the shear key. Effects of positive and negative temperature gradients are shown. It can be noticed that, in general, tensile stresses were decreased as the transverse post-tensioning force increased. Positive temperature gradients have an adverse effect, since it introduces additional stresses in the shear key. It can be seen that negative temperature gradients did not have a considerable effect in the tensile stresses.

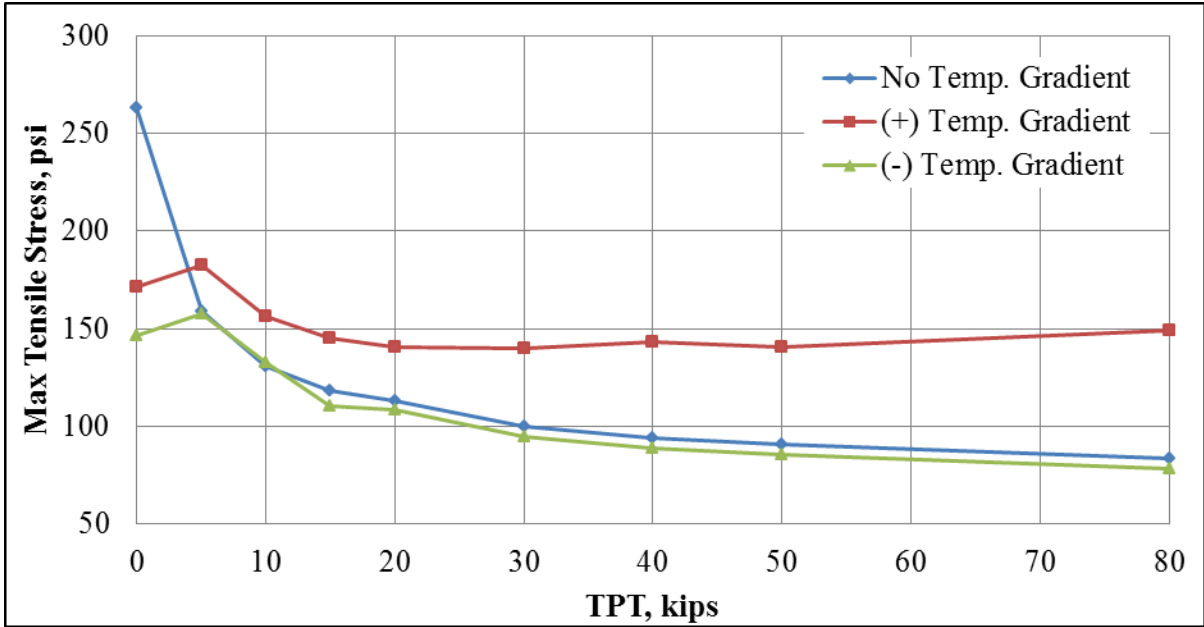


Figure 14 Maximum tensile stress verse TPT

Figure 15 shows the maximum compressive stresses as a function of the transverse post-tensioning force. Results show that a significant increment in the maximum compressive stress in the shear key was obtained when positive temperature gradients were included in the model. The compressive stresses were increased in excess of 40% when the positive temperature gradient was included.

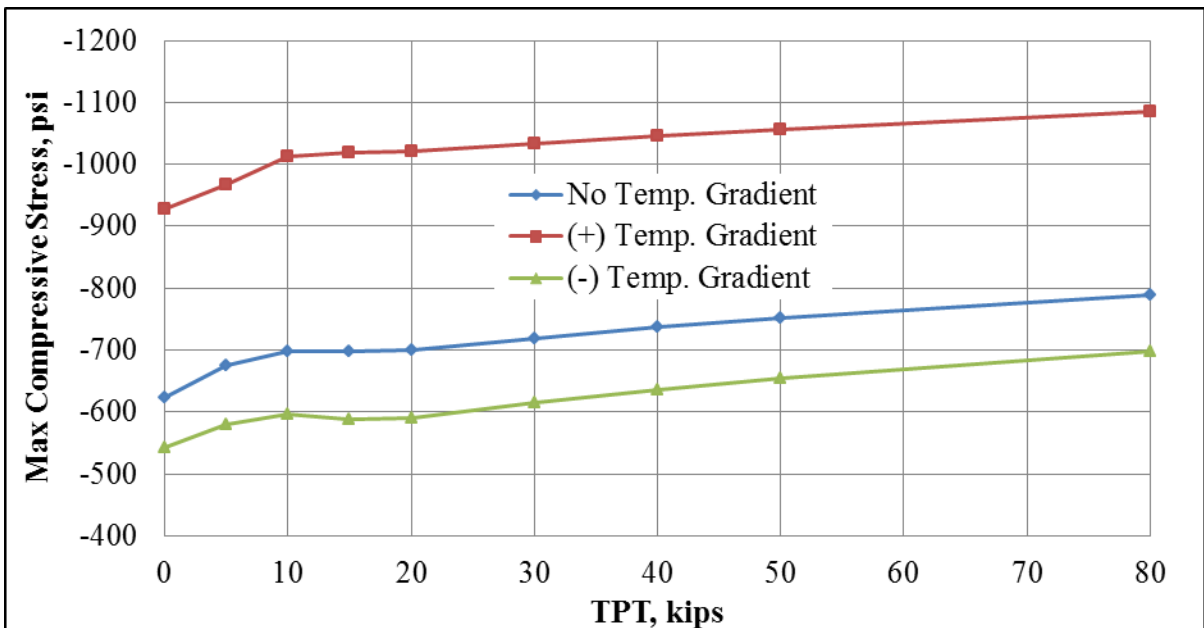


Figure 15 - Maximum compressive stress verse TPT

UHPC MODEL

The results collected from the UHPC model included the deflection of the beams at four nodes (Figure 16). These nodes were at midspan and at the locations of linear variable displacement transducers LVDT's from the FHWA testing. This allowed direct comparison of analytical and experimental results.

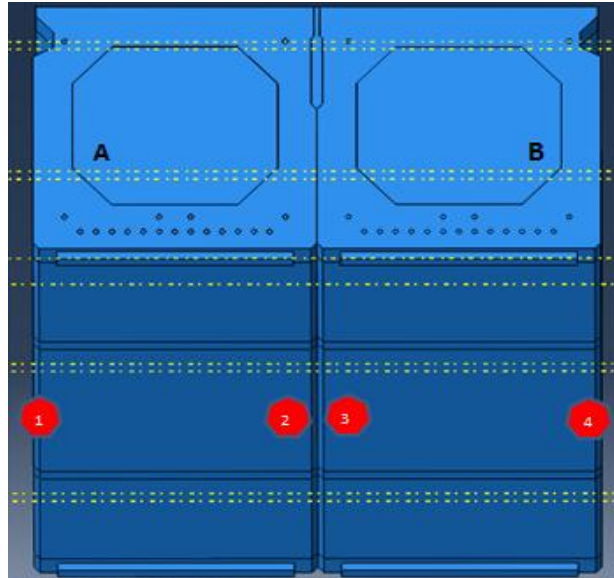


Figure 16: Four deflection nodes that were monitored for deflection during loading

When compared to results from the experimental testing of a composite box beam with a partial-depth shear key filled with conventional grout, the FEM nodal deflection data was very similar (Figure 17). The percentage of difference between the experimental and analytical values at each node ranged from 0.12%-8.69%. As testing of the remaining three beam configurations are completed in the future at TFHRC, more FEM models will be completed and compared.

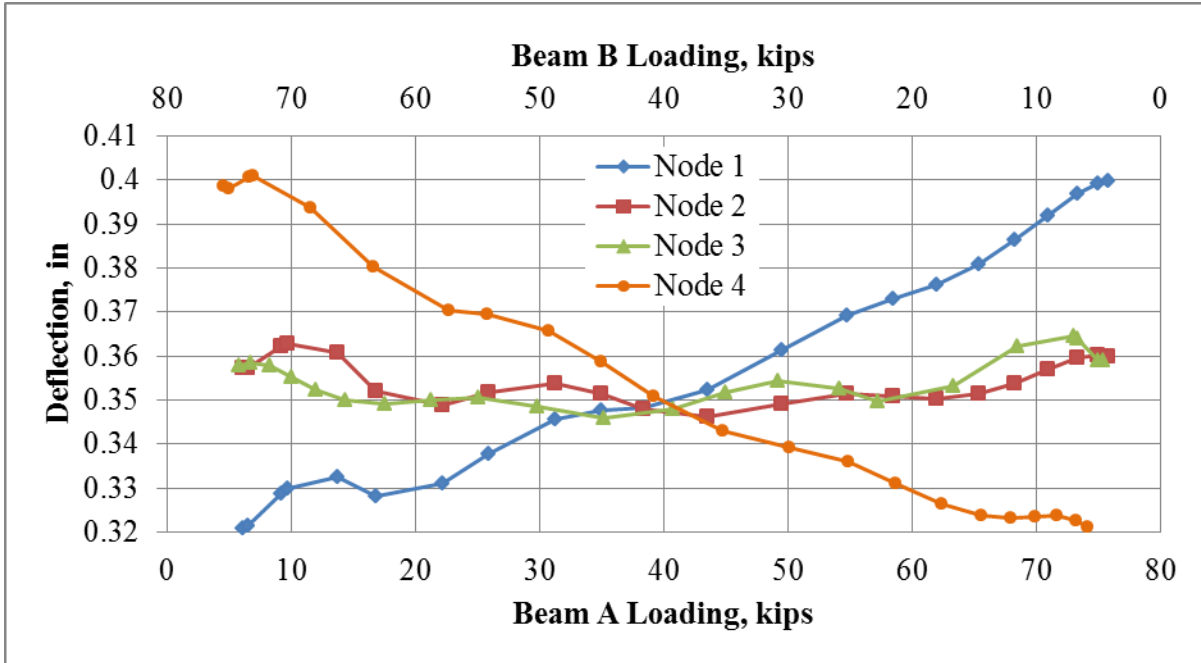


Figure 17 - Nodal deflection data under cyclic loading procedure

SOLLARS ROAD BRIDGE MODEL

The results taken from the finite element model for the Sollars Road Bridge included the deflections on the bottom flange of each of the box beam at midspan and at a third of the span. The deflections were taken at each edge and center across the width of each beam as well. By monitoring the deflections at the edges of the beams, the relative displacement between adjacent beams is more apparent and the transfer of load transverse across the bridge model can be visualized.

To show how the each step of the loading effected the beams, the displacements were reported for the prestressing (PS), the prestressing and the self-weight (DL), and the total loading. The total loading included the prestressing, self-weight, and truck loadings. By subtracting the dead load effects from the total load effects, the live load effects can be shown. Figure 18 shows the deflections results taken from the Sollars Road Bridge model while the trucks were positioned about the center of the bridge at midspan. In the first loading case the center beam was subjected to eight rear axle loads and four front axle loads. This explains why the center beam experiences the largest magnitude of deflection.

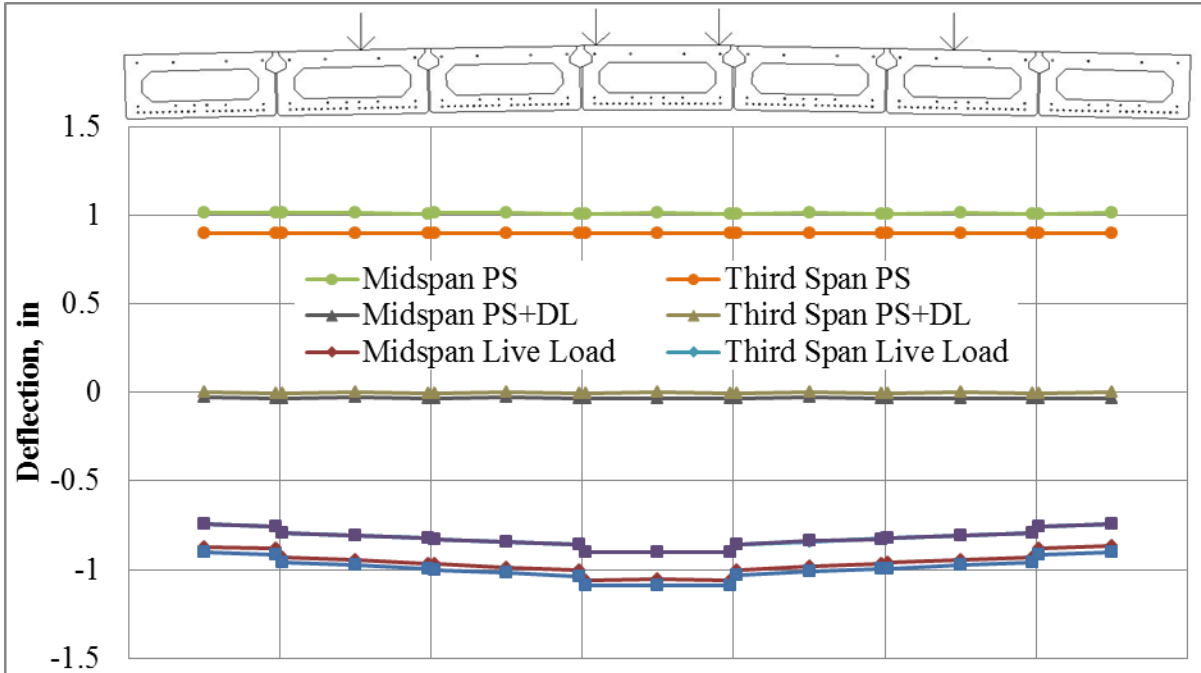


Figure 18 Sollars Road Bridge Model – Truck Loading #1 Deflection Results

Similar to Figure 18, the results while the trucks were positioned to one side of the bridge are shown in Figure 19. As would be expected, the prestressing and dead load had the same effect on the beam deflections prior to being loaded by the trucks. However, it is apparent in the results that the trucks were positioned to one side of the bridge. In Figure 19 the side of the bridge loaded by the truck was displaced the largest by the live loading.

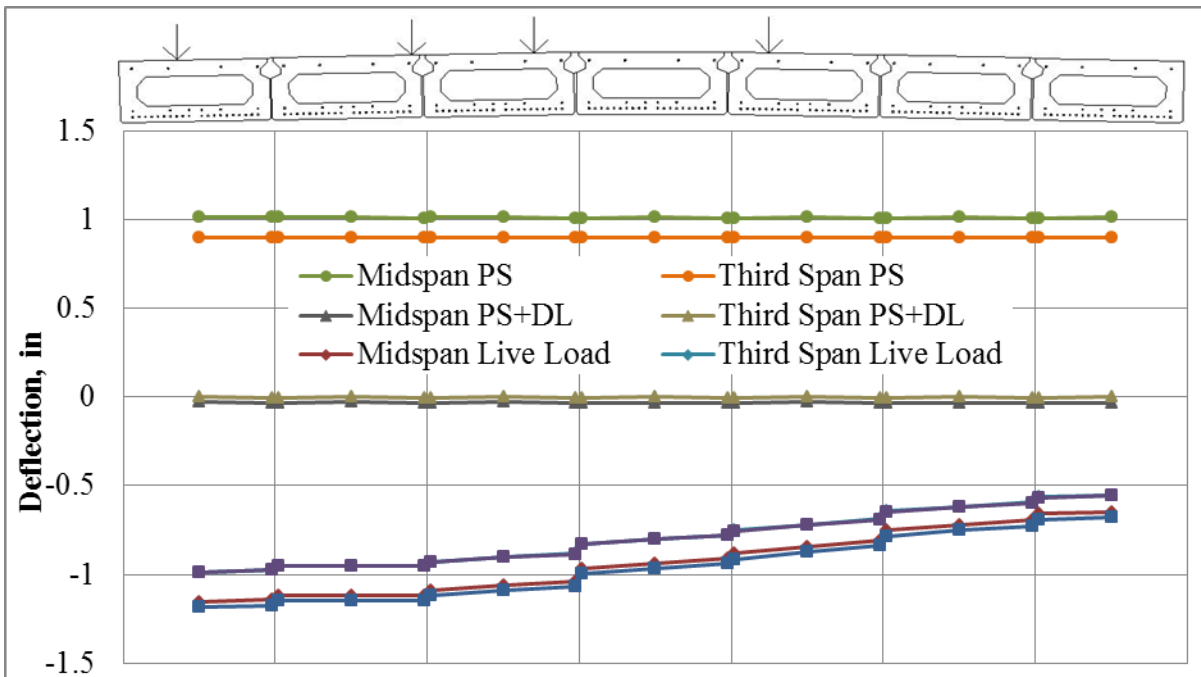


Figure 19: Sollars Road Bridge Model – Truck Loading #2 Deflection Results

As previously discussed, using perfectly plastic material properties for the concrete would not significantly affect the global behavior of the model. The largest tensile strain experienced in the concrete during the first truck loading was approximately $85 \mu\epsilon$. The magnitude of tensile strain expected to cause cracking is approximately $115 \mu\epsilon$. The largest tensile strain experienced in the second truck loading was $128 \mu\epsilon$. However, there were only 8 of the 112,072 elements with concrete material properties exceeded a tensile strain of $115 \mu\epsilon$. There were no concrete elements of the model in that exceeded the yield strain in compression.

CONCLUSIONS:

TEMPERATURE MODEL

Results from the finite element model indicate that, the differential deflections between the two beams decreased as the transverse post-tensioning force increased. If contact between the two box beams was allowed and frictional forces can be developed, a TPT of 10 kips per diaphragm was enough to limit the differential deflections to less than 0.02 in.

When maximum tensile and compressive stresses in the shear key were analyzed, the following conclusions were drawn. In general, maximum tensile stress decreases as the transverse post-tensioning force increases. Also, the maximum compressive stress increases as the transverse post-tensioning force increases. Regardless the amount of TPT, the maximum compressive stresses did not exceed the compressive strength of the grout. Thus, evidence suggests that the dominant failure mode was obtained when the maximum shear stress breaks the bond at the interface between the shear key and the box-beam.

On the other hand, positive temperature gradients contribute significantly to increase the compressive and tensile stresses in the shear key. Based on the results, it can be seen that tensile stresses in the shear key increased by more than 20% when positive temperature gradient was considered. The maximum compressive stresses increased by more than 40% when positive temperature gradients were considered. Negative temperature gradients did not affect the maximum tensile stresses in the shear key, but did decrease the maximum compressive stresses by approximately 15%.

UHPC MODEL

It can be seen from this data that the mechanical behavior of the beams was in accordance with the load application pattern. This is because the beam with the higher applied load was expected to deflect more than the beam with the lower applied load according to Figure 8. The deflection from nodes 2 and 3 also seem to fluctuate around the same general area due to their location closer to the middle of the pair of beams. When analyzing the percent differences between the FEM and TFHRC's results, it was also noticed that node 1's deflection data consistently produced the highest percentage difference, while node 4's deflection data consistently produced the smallest percentage difference. This is

most likely due to the difference in actual stiffness between both beams where the two beams in the FEM were assumed to be identical.

SOLLARS ROAD BRIDGE MODEL

From the initial results of the Sollars Road Bridge model, it can be concluded that the design for the future bridge with the UHPC shear keys will be able to sufficiently transfer load transversely across the bridge. The dowel-in bars and UHPC shear key were able to replace the conventionally grouted shear key and post-tensioned transverse tie bar system.

Once the bridge is completed, minor non-destructive testing on the in-situ bridge will allow for the model to be updated. Knowing the actual strength of the concrete of the superstructure will enable the model to more accurately represent the bridge. After the truck testing is completed, the interaction between the beams and shears keys may be altered to better predict the bridge behavior under different loading conditions.

REFERENCES:

1. Graybeal,. "Finite Element Analysis of UHPC: Structural Performance of an AASHTO Type II Girder and a 2nd-Generation Pi-Girder." *Technical Brief*. November 2010.
2. Wipf, Terry, et al. "Iowa's Ultra-High Performance Concrete Implementation." *Iowa Department of Transportation News* April 2011.
3. Graybeal, B. "Construction of Field-Cast Ultra-High Performance Concrete Connections." *Technical Note*. April 2012.
4. Graybeal, B. "Behavior of UHPC Connections Between Precast Bridge Deck Elements. Federal Highway Administration", 2010.
5. Huffman, J., Steinberg, E., Sargand, S. "Finite Element Modeling a Full Scale Adjacent Prestressed Concrete Box Beam Bridge Span". *PCI/NBC Conference*, October 2012.
6. AASHTO LRFD *Bridge Design Specification Fifth Edition*, American Association of State Highway and Transportation Officials, Sections 3.12.3-1 & 14.7.6.3.3-1, 2010
7. Wan, Z. (2011). *Interfacial Shear Bond Strength Between Old and New Concrete*. Master Thesis. Beijing University of Technology.
8. Wight, J. K., & MacGregor, J. G. (2012). *Reinforced concrete: Mechanics and design*. Upper Saddle River, New Jersey: Pearson Education, Inc.
9. Cook, R.A., Allen, D.T., Ansley, M.H. "Stiffness Evaluation of Neoprene Bearing Pads Under Long Term Loads." *Florida Department of Transportation Report*, March 2009.

10. Barzegar, F., Maddipudi, S. “Three-Dimensional Modeling of Concrete Structures. II: Reinforced Concrete”. *Journal of Structural Engineering*, 1997, pp. 1347-1356.
11. Setty, C. J. (2012). *Truck Testing and Load Rating of a Full-Scale 43-Year-Old Prestressed Concrete Adjacent Box Beam Bridge*. Masters Thesis, Ohio University, Russ College of Engineering and Technology.